Magnolol as an Antibacterial Agent Against Drug-resistant Bacteria Targeting Filamentous Temperature-sensitive Mutant Z

Ning Sun [a,*], Xin Deng [a], Hanqin Kong [a], Ziling Zhi [b], Guli Jiang [a], Jing Xiong [a], Sisi Chen [b], Song Li [c], Wenchang Yuan [b,*], Wing-Leung Wong [d,*]

[a] Guangzhou 11th People's Hospital, Guangzhou Cadre and Talent Health Management Center, Guangzhou, P.R. China.

[b] Guangzhou Key Laboratory for Clinical Rapid Diagnosis and Early Warning of Infectious Diseases, KingMed School of Laboratory Medicine, Guangzhou Medical University, Guangzhou, P. R. China.

[c] Department of Laboratory Medicine, The Second Affiliated Hospital of Guangzhou University of Chinese Medicine, Guangdong Provincial Hospital of Chinese Medicine, Guangzhou, P. R. China

[d] State Key Laboratory of Chemical Biology and Drug Discovery, and Department of Applied Biology and Chemical Technology, The Hong Kong Polytechnic University, Hung Hom, Kowloon, Hong Kong, P. R. China.

* Corresponding author

Email: (N. Sun): ning.sun@connect.polyu.hk

Email: (W. Yuan): yuanwenchang95@163.com

Email: (W. Wong), wing.leung.wong@polyu.edu.hk

Abstract

The emergence of multiple drug-resistant bacteria poses critical health threats worldwide. It is urgently needed to develop potent and safe antibacterial agents with novel bactericidal mechanisms to treat these infections. In this study, magnolol was identified as a potential bacterial cell division inhibitor by a cell-based screening approach. This compound showed good antibacterial activity against a number of Gram-positive pathogens (minimum inhibitory concentration 8–16 μg/mL) including methicillin-resistant Staphylococcus aureus and vancomycin-resistant Enterococcus. Further results obtained from biochemical experiments demonstrated that magnolol could markedly disrupt GTPase activity and filamentous temperature-sensitive mutant Z (FtsZ) polymerization, consistent with the impediment to cell division in the bacteria tested. The in vivo antibacterial activity of magnolol was evaluated with a Galleria mellonella larvae model. The results showed that magnolol significantly increased the survival rate of larvae infected with methicillin-resistant S. aureus. The interaction pattern of magnolol with FtsZ was investigated through molecular docking. The finding may offer meaningful insights into the mechanism of action of the compound. The results point to magnolol as a promising antimicrobial compound that inhibits cell division by affecting FtsZ polymerization and has the potential to be developed into an effective antimicrobial drug by further structure modification.

Keywords:

Bacterial resistance; magnolol; antibacterial activity; cell division; FtsZ inhibitor.

Introduction

Antimicrobial resistance (AMR) arises when microbes, such as bacteria, evolve to defend against antimicrobial drugs [1]. Treating bacterial infections caused by these resistant strains is challenging currently because the effectiveness of most clinically used antibiotics has been largely reduced, leading to a shrinking arsenal of potent medications [2]. In recent years, AMR has emerged as a big challenge worldwide and poses a high risk to public health [3]. Prominent examples of antibiotic-resistant bacteria including vancomycin-resistant Enterococcus (VRE) and methicillin-resistant Staphylococcus aureus (MRSA) have been reported [4]. Hence, there is an urgent need to develop new and effective strategies to combat drug-resistant bacterial infections [5].

Given the crucial function and conserved nature of filamentous temperature-sensitive mutant Z (FtsZ) in the division of bacterial cells, it has emerged as a promising target for the discovery of novel antibacterial agents [6]. During bacterial cell division, FtsZ needs to undergo assembly to form a circular structure called Z-ring at the division site [7]. This assembly process involves GTP binding and hydrolysis. Subsequently, FtsZ is stabilized and then attaches to the inner surface of the cytoplasmic membrane through interactions with FtsZ-binding proteins. When the Z-ring is established, FtsZ starts to recruit other proteins that initiate cytokinesis [8]. It is generally believed that potent FtsZ inhibitors could suppress this critical biological process during bacterial cell division. Cells that are deficient in functional FtsZ are unable to divide and instead grow into long filaments (rod-shaped bacteria) or enlarged cocci (cocci-shaped bacteria) that eventually lyse [9].

Naturally occurring compounds may offer several advantages in the discovery of new drugs because they often exhibit low toxicity and minimal side effects [10]. Recently, some natural products including curcumin, berberine, and plumbagin have been reported to be able to target FtsZ (Figure 1) [9]. These compounds were found able to inhibit bacterial growth for some strains such as S. aureus, Enterococcus faecium, and Bacillus subtilis via the mechanism of inhibiting bacterial cell division by disrupting FtsZ function with the compound [11]. In the present study, we conducted a cell-based screening assay to evaluate a small library of natural products in order to search for lead compounds to inhibit bacterial cell division, and we identified a small biphenyldiol compound, magnolol, that was found in Magnolia officinalis [12]. This natural compound was found for the first time showing potent inhibitory effects against bacterial cell division. We thus

conducted an in-depth investigation to understand its antibacterial properties against a range of bacterial species and the antibacterial mechanism. The results show that magnolol may be able to inhibit bacterial division and growth by interrupting the biofunction of FtsZ.

2 Materials and Methods

2.1 Materials

Magnolol (Cat. No.: S2321, purity 99.95%) and berberine chloride (Cat. No.: S2271, purity 99.75%) used in this project were purchased from Selleck (www.selleck.cn). Dimethyl sulfoxide (DMSO) was utilized to prepare stock solutions, with a consistent final concentration of 1% (v/v) in all assays conducted. The bacterial strains *B. subtilis* 168, *S. aureus* ATCC 29213, ATCC 29247, ATCC 33591, ATCC 33592, and ATCC 43300, *Staphylococcus epidermidis* ATCC 12228, *Enterococcus faecalis* ATCC 29212 and ATCC 51575, *E. faecium* ATCC 49624 and ATCC 700221, *Escherichia coli* ATCC 25922, *Pseudomonas aeruginosa* ATCC BAA-2108 and *Klebsiella pneumoniae* ATCC BAA-1144 used in this research were purchased from American Type Culture Collection (ATCC, USA). Other clinically isolated strains are available in our in-house collection and were identified according to our previous report [13]. The isolation of these strains from clinical samples was approved by the Ethics Committee of Guangdong Provincial Hospital of Chinese Medicine (No. ZM2019-280).

2.2 Cell-Based Cell Division Inhibitory Screening Assay

The experiment was performed according to previously reported methods [14]. *B. subtilis* 168 ATCC 23857 cells were cultured in a starvation medium containing 1% hydrolyzed casein (Sigma) for overnight incubation. Subsequently, the culture was diluted to an optical density (OD_{600}) of approximately 0.01 in a starvation medium with 3% hydrolyzed casein, and the cells were incubated at 37°C. A stationary phase culture was further diluted to an OD_{600} of about 0.06, and 10 μL aliquots were transferred into 96-well microtiter plates that contained various concentrations of screening compounds in 100 μL of the medium. After approximately 5 h of incubation at 37°C, the cell morphology was examined using phase-contrast light microscopy. Berberine, a natural compound known to inhibit *B. subtilis* cell division at a concentration of 64 μg/mL [11], was employed as a positive control in this assay. Each condition was replicated three times. Compounds showing inhibition of *B. subtilis* cell division at concentrations lower than 64 μg/mL were selected for further investigation.

2.3 Antimicrobial Susceptibility Test

All strains utilized in this study were obtained from the American Type Culture Collection (ATCC, USA), or clinical isolated strains already available in. our group. The mediums used for bacterial culture are purchased from BD Difco, USA. The minimum inhibitory concentrations (MICs) of magnolol against the tested strains were determined in accordance with the protocols outlined in the Clinical and Laboratory Standards Institute (CLSI) guidelines [15]. *S. aureus* strains were grown in Cation-adjusted Mueller Hinton broth (CA-MHB), while *E. faecalis* and *E. faecium* strains were cultivated in Brain Heart Infusion (BHI) broth. The remaining strains were cultured in MHB for the assays. The MIC was defined as the lowest concentration of the compound that inhibits the visible growth of the bacteria. Methicillin and berberine were used as controls in this assay. Each strain was tested three times to ensure reproducibility.

2.4 Minimum Bactericidal Concentration Assay

The described protocol was employed to assess the minimum bactericidal concentration (MBC) of an antibacterial agent, which is critical in determining whether the compound is bactericidal. To determine the MBC, 10 μL of the culture from the MIC assay was plated onto agar plates: CA-MHB agar for *S. aureus* strains, MHB agar for *B. subtilis*, and BHI agar for *E. faecium*. These plates were then incubated at 37°C. After a 24-h incubation period, the plates were examined for colony formation. The MBC was recorded as the lowest concentration of the compound that prevented the formation of bacterial colonies [16]. This test was replicated three times for each strain to ensure accuracy.

2.5 Time-Killing Curve Determination

Time-killing curves of magnolol against selected bacteria were performed according to our previous study [17]. The assay aimed to evaluate the dynamics of magnolol's antibacterial activity. Overnight cultures of tested strains were diluted to an approximate concentration of 10^5 CFU/mL. Various concentrations (1×MIC, 2×MIC, and 4×MIC) of magnolol were introduced into the bacterial suspensions. These mixtures were then incubated at 37°C with a rotational speed of 250 rpm. At specified time intervals (0, 2, 4, 6, 8, and 24 h), 100 μL of the culture was removed and subjected to serial dilutions. These dilutions were subsequently spread onto CA-MHB or MHB agar plates. After an additional 24-h incubation at 37°C, the number of viable cells (CFU/mL) was recorded. This process was repeated three times for each time point to ensure the reliability of the data.

2.6 Light Scattering Assay

The preparation of *S. aureus* FtsZ followed a previously established methodology [14]. For the light scattering assay, FtsZ at a concentration of 6 μM was mixed with varying concentrations (2, 4, and 8 μg/mL) of magnolol at room temperature and allowed to incubate for 10 min. Subsequently, a solution containing 20 mM KCl, 5 mM $MgCl_2$, and 1 mM GTP was added, and the resulting mixture was immediately analyzed for light scattering by a temperature-controlled (37°C) fluorescence spectrometer. In this assay, 1% DMSO and 5 μg/mL methicillin were used as the vehicle and negative control, respectively.

2.7 GTPase Activity Assay

The GTPase activity assay was performed in accordance with previously published methods that investigated the effect of magnolol on FtsZ GTPase activity [18]. Briefly, 3.5 μM of FtsZ was mixed with varying concentrations of magnolol (0, 2, 4, 8, 16, and 32 μg/mL) in a 20 mM Tris buffer at room temperature. Following a 10-minute incubation, 5 mM $MgCl_2$, 200 mM KCl, and 500 mM GTP were introduced to the reactions. The mixtures were then incubated at 37°C for an additional 30 min. To stop the reactions, 100 μL of Cytophos reagent (BK054; Cytoskeleton) was added, and the mixture was incubated for another 10 min. Inorganic phosphate production was measured quantitatively using a microplate reader at a wavelength of 650 nm.

2.8 Molecular Docking Study

Molecular docking was conducted utilizing Discovery Studio (DS) 2016. An X-ray crystal structure of *Sa*FtsZ was retrieved from the Protein Data Bank (PDB code: 4DXD) [19]. Within DS, both FtsZ and the ligand magnolol were prepared for the investigation. Subsequently, the CDocker

protocol was employed to forecast the binding conformations, with the most favorable poses being examined visually.

2.9 Visualization of *S. aureus* Morphology

S. aureus ATCC 43300 was incubated in a CA-MHB medium. The bacterial cells were then diluted to 1×10^5 CFU/mL and combined with the absence or different concentrations of magnolol. After shaking at 37°C for 4 h, the cells were harvested and re-suspended in phosphate buffer solution. Next, 3 μL of bacterial suspension was added to a microscope slide that had been pre-treated with 0.1% (w/v) poly-L-lysine. The morphology of *S. aureus* was observed at 400× magnification, and the images were captured using an Olympus IX71 microscope.

2.10 The Evaluation of Magnolol Activity with an MRSA-Infected *G. mellonella* Larvae Model

Approximately 0.25 g of larvae were randomly assigned to different groups. These groups were tested under the following conditions: control group (vehicle), phosphate-buffered saline (PBS) (0.5% DMSO), infected group (injected with MRSA (*S. aureus* ATCC 43300) suspensions to achieve a final concentration of 0.5 McFarland), magnolol compound group (injected with magnolol at doses of 8 or 32 μg/mL), and treatment group (injected with magnolol at doses of 8 or 32 μg/mL 2 h after *S. aureus* injection). Each larva in the group was injected with a solution of magnolol, containing 20 μL, using a microinjector (HAMILTON, Swiss). After injections, the larvae were kept in a dark room at 37°C. The number of viable larvae in each experimental group was counted every 24 h for a duration of 120 h. Then, the survival rates were calculated and represented graphically [20]. Statistical analysis and graphical representation of the results were conducted using GraphPad Prism 8.0 software (GraphPad Software, San Diego, California, USA). The data were presented as the mean ± standard deviation (x ± s). The significance assessment was performed using the Log-rank test; statistical significance was denoted by $p < 0.05$, with $*p < 0.05$, $**p < 0.01$, and $***p < 0.001$ indicating varying degrees of significance.

3 Results

3.1 Cell Division Inhibitory Effect of Magnolol on *B. subtilis*

To identify active compounds with good inhibitory activity against bacteria, we utilized cell-based screening assays to screen commercially available phenol-containing compounds for their antibacterial potential by following the reported procedures [14]. Our preliminary results obtained from the screening study identified a natural compound, magnolol (molecular mass: 266.3 g/mol), which was able to induce a notable lengthening of *B. subtilis* cells when magnolol was applied at 8 μg/mL. The *B. subtilis* cells without magnolol treatment exhibited a characteristic rod shape with a short length ranging from 5 to 15 μm (Figure 2A). When the cells were incubated with 8 μg/mL magnolol, an elongation of the cell exceeding 50 μm was observed (Figure 2B). This effect is found similar to the *B. subtilis* cells that were treated with berberine at 64 μg/mL (Figure S1). These observations are also in agreement with the effects found with the use of FtsZ inhibitors such as pyrimidine and benzamide derivatives [18, 21]. Thus, the results suggest that magnolol may potentially interrupt the FtsZ function and cause abnormal cell division. We thus further studied the effect of magnolol on FtsZ activity.

3.2 Antibacterial Activity of Magnolol

We evaluated the antibacterial activity of magnolol against a number of clinically relevant bacterial strains including several drug-resistant bacteria. Our results revealed that magnolol efficiently

inhibited the growth of all Gram-positive bacteria strains tested (Table 1). The MIC values of magnolol were found in the range of 8–16 μg/mL. The antibacterial results of magnolol against drug-sensitive Gram-positive strains showed that the growth of *S. aureus* ATCC 29213, *B. subtilis* 168, and *Staphylococcus epidermidis* ATCC 12228 was suppressed by magnolol at 8 μg/mL. The antibacterial activity of magnolol against the above-mentioned strains is slightly lower than that of methicillin and it is more potent than that of berberine (>96 μg/mL). Moreover, compared to methicillin and berberine, magnolol exhibits a markedly stronger antibacterial effect against MRSA (Table 1).

Next, we assessed magnolol against 50 clinical isolates of MRSA (Table S1). Our results indicated that magnolol showed potent antibacterial activity against all these clinical MRSA with MIC values obtained down to 8 μg/mL (Table S1). We also tested the antibacterial activity of magnolol against *E. faecalis* and *E. faecium*. It was found that magnolol effectively inhibited the growth of *E. faecalis* and *E. faecium*, including the vancomycin-resistant strains (VREs), with a MIC value of 16 μg/mL (Table 1). Nonetheless, for Gram-negative bacteria such as *Escherichia coli*, *Pseudomonas aeruginosa*, and *Klebsiella pneumonia*, magnolol at 64 μg/mL showed no observable antibacterial activity. This could be attributed to the outer membrane barrier or efflux pumps of Gram-negative bacteria that may efficiently prevent magnolol from penetrating into the bacterial cells [22].

3.3 Bactericidal Test of Magnolol Against the Selected Bacterial Strains

Having evaluated the antibacterial activity of magnolol against the clinically relevant bacteria, we then investigated whether the killing effect of magnolol is bactericidal or bacteriostatic. For this purpose, we determined the minimum bactericidal concentrations (MBCs) of magnolol against *B. subtilis* 168, *S. aureus* ATCC 29213, *S. aureus* ATCC 43300 (MRSA), and *E. faecium* ATCC 700221 (VRE) (Table 2). According to the guidelines set forth by the CLSI [23], an MBC/MIC ratio of 1–2 is indicative of bactericidal activity. Our results clearly indicate that all the MBC/MIC ratios obtained are not higher than 2, suggesting that magnolol may possess bactericidal activity against the bacterial strains tested.

3.4 Kinetics of the Bactericidal Activity of Magnolol

After having validated the bactericidal property of magnolol, we performed experiments to obtain time-killing curves to understand the dynamic of its bactericidal activity against *S. aureus* ATCC 43300, *B. subtilis* 168, *S. aureus* ATCC 29213, and *E. faecium* ATCC 700221. As depicted in Figure 3A, S. *aureus* ATCC 43300 without magnolol treatment exhibited rapid growth for the initial 6 h. After 6 h, the growth curve of *S. aureus* was found to level off, indicating that the bacteria may be under a stationary phase.

When *S. aureus* ATCC 43300 was incubated with magnolol at the concentrations of 2 × MIC and 4 × MIC, it was found that the bacterial growth was completely inhibited. Magnolol at 1 × MIC was also able to reduce *S. aureus* colony-forming units per milliliter to below 10^3 CFU mL^{-1} after 24-h incubation. The observation of bacterial growth inhibition across different concentrations of magnolol revealed a remarkable dose-dependent killing rate for *S. aureus* ATCC 43300 (Figure 3A). A comparable trend was also observed when the other three strains were treated with magnolol over 24-h monitoring (Figure 3B and Figure S2). However, the growth of *B.*

subtilis and *E. faecium* was completely inhibited with magnolol treatment at the MIC level (Figure 3B and Figure S2), which was found better than that of *S. aureus*. These findings were consistent with the results obtained from MBC tests. The results may also further support that magnolol has a bactericidal effect on these bacteria.

3.5 Effects of Magnolol on the FtsZ Activity

We then further explored the effect of magnolol on the biological function of FtsZ because it could be a potential target of the compound. The light scattering assays were applied to detect whether magnolol could disrupt the dynamic polymerization of FtsZ. The assays were performed with magnolol at a concentration range from 2 to 8 μg/mL. Figure 4A presents the dynamic polymerization kinetics of FtsZ under the conditions with and without the addition of magnolol. The results shown in Figure 4A clearly demonstrated that magnolol enhanced FtsZ polymerization in a dose-responsive manner. This behavior is consistent with the effects observed in other FtsZ-targeting compounds reported previously [24]. In the assays, methicillin was used as a negative control under the same conditions. The results clearly indicated that methicillin did not interrupt the polymerization activity of FtsZ because it was not the drug target of methicillin.

The rate at which GTP is being hydrolyzed has been known associated with the dynamic assembly and disassembly of FtsZ [8]. To understand whether the antibacterial mechanism of magnolol could be a possible action of its inhibitory effects on GTPase activity, we thus studied the impact of magnolol on the GTPase function of FtsZ. We found that magnolol was able to inhibit FtsZ GTPase activity in a concentration-dependent manner (Figure 4B). The GTPase activity was inhibited by 18%, 42%, 58%, 78%, and 81% with magnolol at 2, 4, 8, 16, and 32 μg/mL, respectively. The results suggest that magnolol may be able to inhibit GTPase activity and consequently, the compound may disrupt the polymerization of FtsZ and potentially inhibit bacterial cell division.

3.6 Predicted the Binding Mode of Magnolol in FtsZ Protein

To explore further the possible interaction of magnolol with FtsZ, a molecular modeling study using Discovery Studio (DS) was performed to predict the potential binding sites and mode of magnolol-FtsZ interactions. The optimal docking pose suggests that the magnolol could likely bind to a hydrophobic and narrow groove composed of the T7-loop, H7-helix, and a four-stranded β-sheet (**Figure** 5A). A 2-dimensional magnolol-FtsZ interaction diagram shown in **Figure** 5B displays the potential interactions between magnolol and the amino acid residues of FtsZ. The hydrophobic interactions are found crucial for magnolol binding to the key residues of FtsZ, which include Asp 199, Leu 200, Val 203, Met 226, Val 297, Thr 309, and Ile 311. Particularly, a π-lone pair interaction was observed between Thr 309 and the aromatic ring of magnolol. Moreover, the van der Waals force may also participate in the interaction between magnolol and some amino acids such as Val 307, Gly 227, and Gly 205, which are located in the immediate vicinity of the binding pocket. The information obtained through predicting magnolol-FtsZ molecular interactions may offer insights for guiding further structural advancement based on the molecular scaffold of magnolol and developing potent and FtsZ-specific molecular inhibitors.

3.7 Effects of Magnolol on the Morphology of *S. aureus* Cells

To further explore the antibacterial mechanism of magnolol, *S. aureus* ATCC 43300 was used to evaluate the bacterial cell division inhibitory effect of magnolol. The diameter of bacterial cells observed in the control group was about 1 μm, while after treating with magnolol at 8 μg/mL, an

enlargement of cell size was observed clearly (**Figure** 6). These results indicate that the compound may target FtsZ and exert significant effects on the inhibition of bacterial cell division.

3.8 In Vivo Antibacterial Activity of Honokiol

We also evaluated the in vivo toxicity and antibacterial activity of magnolol. A *Galleria mellonella* larvae model, a widely used non-mammalian system for antibacterial drugs [25], was utilized for a preliminary evaluation. Our results showed that the survival rates of the larvae treated with magnolol at 8 and 32 μg/mL were 96.6% and 93.1%, respectively, after incubation for 120-h (**Figure** 7). These in vivo toxicity results did not show a statistically significant difference compared to the control (without any treatment) and PBS groups ($p_1 = 0.5480$, $p_2 = 0.2945$). The results suggest that magnolol may have low or no toxicity against larvae. In contrast, the survival rate of larvae infected with MRSA (*S. aureus* ATCC 43300) dropped dramatically to 6.9% after 120 h. When the larvae infected with MRSA were treated with magnolol (at 8 and 32 μg/mL), a substantially higher survival rate was observed at 120-h. The survival rates for these infected larvae treated with 8 and 32 μg/mL magnolol were 75.9% ($p = 0.0103$) and 89.6% ($p < 0.0001$), respectively (**Figure** 7). This markedly improved survival rate not only indicates statistical significance but also demonstrates the efficacy of magnolol in rescuing larvae from MRSA infection.

4 Discussion

In recent years, accumulating evidence indicates that magnolol exhibits a broad spectrum of pharmacological activities [12, 26]. For example, magnolol shows anti-inflammatory effects by inhibiting the Toll-like receptor 2 (TLR2), TLR4, NF-κB, MAPK, and peroxisome proliferator-activated receptor-γ (PPAR-γ) pathways, as well as by reducing the expression of inflammatory cytokines [27]. Additionally, numerous studies have shown that magnolol possesses antitumor activity against a variety of cancers, including melanoma [28], cholangiocarcinoma [29], oral cancer [30], colon cancer [31], prostate cancer [32], and lung cancer [33]. This compound was found to inhibit the growth, migration, and invasion of tumor cells, and was able to promote apoptosis and autophagy. These effects are mediated through its action on caspase-8, caspase-3, and other proteins involved in the p53, MAPK, NF-κB, TLR, HIF-1α/VEGF, PI3K/Akt/ERK/mTOR, and Wnt/β-catenin signaling pathways [33, 34]. Last but not least, magnolol demonstrates hypoglycemic activity and inhibits protein tyrosine phosphatase 1B (PTP1B) by modulating the AMPK/SIRT1/PGC-1α, PPAR-γ, and PKA pathways. It enhances the activity of glyoxalase 1, PDX1, Ins2, and GPX genes. It also stimulates Akt phosphorylation and inhibits α-glucosidase [35].

According to a literature review, magnolol possesses antibacterial properties [26]. It has been shown to inhibit *Aeromonas hydrophila* strains with MIC values ranging from 32 to 64 μg/mL [36]. Sakaue et al. reported that magnolol inhibited *Streptococcus mutans*, helping to prevent dental caries, with a MIC value of 10 μg/ml. Additionally, magnolol at 50 μg/ml exhibited superior bactericidal activity against *S. mutans* biofilm compared to chlorhexidine at 500 μg/ml, and the antibacterial effect was rapid and was just 5 min after treatment [37]. Oufensou et al. evaluated the antifungal activities of magnolol (at concentrations ranging from 5 to 400 μg/mL) against 32 *Fusarium spp*. strains, using terbinafine (0.1-10 μg/ml) and fluconazole (1-50 μg/ml) as positive controls. The results indicated that magnolol exhibited bactericidal activity comparable to that of

fluconazole [38]. However, the antibacterial mechanism of magnolol is still not clear and further investigation is needed.

In this study, we found that magnolol possesses good antibacterial activity against the tested Gram-positive bacteria including MRSA and VRE. The MIC values obtained are in the range of 8-16 μg/mL, which is similar to or even better than the natural products that were reported for FtsZ-targeting. For instance, berberine inhibited the growth of MRSA with MIC values of 112-196 μg/mL. Its synthesized 9-phenoxyalkyl derivatives were suggested to bind to the C-terminal interdomain cleft of FtsZ and inhibit the growth of MRSA and VRE with MIC values of 2–8 and 4–16 μg/mL, respectively [11]. Plumbagin, a naturally occurring naphthoquinone from *Plumbago rosea*, was reported as a potent antimicrobial agent against *S. aureus* with a MIC of 5 μg/mL [39]. Curcumin, one of the major active ingredients of turmeric extract, was reported to inhibit the growth of MRSA and VRE in the concentration range of 128–512 μg/mL [40]. Cinnamaldehyde, an aromatic compound isolated from the stem bark of *Cinnamomum cassia*, was found able to inhibit the growth of MRSA at 250 μg/mL by inhibiting the activity of FtsZ [41]. However, most of the natural-based FtsZ inhibitor, including magnolol, has no antibacterial activity against the tested Gram-negative strain at the concentration of 64 μg/mL, likely owing to the intrinsically lower permeability of the Gram-negative cell membrane [42].

Based on the results obtained from biological assays, we observed that magnolol promoted the polymerization of FtsZ and also inhibited the GTPase activity of FtsZ. This effect is reminiscent of some FtsZ inhibitors, such as quinoline derivatives and PC190723, which have shown similar biochemical outcomes [43]. The polymerization of FtsZ is known to be modulated by its GTPase function, with the accumulation of FtsZ polymers potentially causing a conformational shift to a high-affinity state that facilitates FtsZ assembly [44]. Furthermore, akin to other compounds known to target FtsZ [9], magnolol demonstrates a potent inhibitory impact on bacterial cell division. Our research group has recently disclosed a series of small-molecule compounds that specifically target FtsZ and exhibit potent antibacterial properties, including derivatives of berberine, pyrimidine, and quinolinium [11, 17, 18, 24]. Unfortunately, the toxicity of these compounds hindered their further investigation in animal study. We expect that magnolol, exhibiting low toxicity in the *G. mellonella* larvae model, may possibly overcome the aforementioned issues and could be carried on for in vivo antibacterial investigations in animal models.

5 Conclusions

In conclusion, magnolol was reported for the first time as a potential bacterial cell division inhibitor with antibacterial function by using a cell-based screening method. The compound was also found active in disrupting the assembly and GTPase activity of FtsZ. These effects may thus suppress bacterial cell division. Moreover, magnolol demonstrated a strong antibacterial activity against a number of Gram-positive pathogens including drug-resistant strains MRSA and VREF. Given its attractive antibacterial activity and low toxicity observed in a *G. mellonella* larvae model, magnolol shows great potential to be a lead compound for structural advancements to further enhance its antibacterial efficacy for treating drug-resistant infections.

Acknowledgments

This work was supported by Medical Science and Technology Research Fund of Guangdong Province (project No. A2024177), Guangdong Basic and Applied Basic Research foundation

(project No. 2020A1515011326 and 2021A1515011360), Health and Medical Research Fund (HMRF), Hong Kong SAR (project no. 22210412), Guangdong Province Regional Joint Fund-Youth Fund Project (project No. 2021A1515110857), Guangzhou Municipal School (College) Joint Funding (project No. 2024A03J0026).

Conflicts of Interest

The authors declare no conflicts of interest.

References

1. M. A. Cook and G. D. Wright, "The Past, Present, and Future of Antibiotics," *Science Translational Medicine* **14**, no. 657 (2022): eabo7793.
2. a) L. Bo, H. Sun, Y. D. Li, et al., "Combating Antimicrobial Resistance: The Silent War," *Frontiers in Pharmacology* **15** (2024): 1347750. b) X. Li, Y. Wu, T. Jiang, et al., "China's Plan to Combat Antimicrobial Resistance," *Science* **383**, no. 6690 (2024): 1424–1425.
3. S. Amann, K. Neef, and S. Kohl, "Antimicrobial Resistance (AMR)," *European Journal of Hospital Pharmacy* **26**, no. 3 (2019): 175–177.
4. a) M. Vestergaard, D. Frees, and H. Ingmer, "Antibiotic Resistance and the MRSA Problem," *Microbiology Spectrum* **7**, no. 2 (2019). b) M. Terentjeva, J. Kibilds, J. Avsejenko, A. Cirulis, L. Labecka, and A. Berzins, "Antimicrobial Resistance in *Enterococcus* spp. Isolates From Red Foxes (*Vulpes vulpes*) in Latvia," *Antibiotics* **13**, no. 2 (2024): 114.
5. F. Ruggieri, N. Compagne, K. Antraygues, M. Eveque, M. Flipo, and N. Willand, "Antibiotics With Novel Mode of Action as New Weapons to Fight Antimicrobial Resistance," *European Journal of Medicinal Chemistry* **256** (2023): 115413.
6. a) N. Silber, C. L. Matos de Opitz, C. Mayer, and P. Sass, "Cell Division Protein FtsZ: From Structure and Mechanism to Antibiotic Target," *Future Microbiology* **15** (2020): 801–831. b) A. Casiraghi, L. Suigo, E. Valoti, and V. Straniero, "Targeting Bacterial Cell Division: A Binding Site-Centered Approach to the Most Promising Inhibitors of the Essential Protein FtsZ," *Antibiotics* **9**, no. 2 (2020): 69.
7. D. S. Weiss, "Bacterial Cell Division and the Septal Ring," *Molecular Microbiology* **54**, no. 3 (2004): 588–597.
8. a) J. M. Monteiro, A. R. Pereira, N. T. Reichmann, et al., "Peptidoglycan Synthesis Drives an FtsZ-Treadmilling-Independent Step of Cytokinesis," *Nature* **554**, no. 7693 (2018): 528–532. b) X. Yang, Z. Lyu, A. Miguel, R. McQuillen, K. C. Huang, and J. Xiao, "GTPase Activity–Coupled Treadmilling of the Bacterial Tubulin FtsZ Organizes Septal Cell Wall Synthesis," *Science* **355**, no. 6326 (2017): 744–747. c) A. W. Bisson-Filho, Y. P. Hsu, G. R. Squyres, et al., "Treadmilling by FtsZ Filaments Drives Peptidoglycan Synthesis and Bacterial Cell Division," *Science* **355**, no. 6326 (2017): 739–743.
9. K. A. Hurley, T. M. Santos, G. M. Nepomuceno, V. Huynh, J. T. Shaw, and D. B. Weibel, "Targeting the Bacterial Division Protein FtsZ," *Journal of Medicinal Chemistry* **59**, no. 15 (2016): 6975–6998.
10. a) M. T. Islam, C. Sarkar, D. M. El-Kersh, et al., "Natural Products and Their Derivatives Against Coronavirus: A Review of the Non-Clinical and Pre-Clinical Data," *Phytotherapy Research* **34**, no. 10 (2020): 2471–2492. b) X. Liu, C. Ma, Z. Liu, and W. Kang, "Natural Products: Review for Their Effects of Anti-HBV," *BioMed Research International* **2020** (2020): 3972390.

11. a) D. Rai, J. K. Singh, N. Roy, and D. Panda, "Curcumin Inhibits FtsZ Assembly: An Attractive Mechanism for its Antibacterial Activity," *Biochemical Journal* **410**, no. 1 (2008): 147–155. b) S. Kaur, N. H. Modi, D. Panda, and N. Roy, "Probing the Binding Site of Curcumin in *Escherichia coli* and *Bacillus subtilis* FtsZ—A Structural Insight to Unveil Antibacterial Activity of Curcumin," *European Journal of Medicinal Chemistry* **45**, no. 9 (2010): 4209–4214. c) P. N. Domadia, A. Bhunia, J. Sivaraman, S. Swarup, and D. Dasgupta, "Berberine Targets Assembly of *Escherichia coli* Cell Division Protein FtsZ," *Biochemistry* **47**, no. 10 (2008): 3225–3234. d) N. Sun, F.-Y. Chan, Y.-J. Lu, et al., "Rational Design of Berberine-Based FtsZ Inhibitors With Broad-Spectrum Antibacterial Activity," *PLoS ONE* **9**, no. 5 (2014): e97514.eA. e) . B. Bhattacharya, P. Jindal, A. Singh, D. Datta, and Panda, "Plumbagin Inhibits Cytokinesis in *Bacillus subtilis* by Inhibiting FtsZ Assembly—A Mechanistic Study of Its Antibacterial Activity," *FEBS Journal* **280**, no. 18 (2013): 4585–4599.
12. Y. Lin, Y. Li, Y. Zeng, et al., "Pharmacology, Toxicity, Bioavailability, and Formulation of Magnolol: An Update," *Frontiers in Pharmacology* **12** (2021): 632767.
13. S. Li, D. Han, X. Chen, et al., "Evaluation of the Zybio EXS3000 Mass Spectrometry in Routine Identification of Clinical Isolates," *Heliyon* **9**, no. 8 (2023): e18990.
14. a) N. R. Stokes, J. Sievers, S. Barker, et al., "Novel Inhibitors of Bacterial Cytokinesis Identified by a Cell-Based Antibiotic Screening Assay," *Journal of Biological Chemistry* **280**, no. 48 (2005): 39709–39715. b) W. Yuan, Z. Yu, W. Song, et al., "Indole-Core-Based Novel Antibacterial Agent Targeting FtsZ," *Infection and Drug Resistance* **12** (2019): 2283–2296.
15. M. P. Weinstein, J. B. Patel, C. A. Burnham, S. Campeau, and P. S. Conville, *D. C. Methods for Dilution Antimicrobial Susceptibility Tests for Bacteria That Grow Aerobically*, Wayne, PA: Clinical and Laboratory Standards Institute, (2018).
16. Z. Zheng, N. Tharmalingam, Q. Liu, et al., "Synergistic Efficacy of Aedes aegypti Antimicrobial Peptide Cecropin A2 and Tetracycline Against *Pseudomonas aeruginosa*," *Antimicrobial Agents and Chemotherapy* 7 (2017): e00686-17.
17. D. X. Zhong, M. T. She, X. C. Guo, et al., "Design and Synthesis of Quinolinium-Based Derivatives Targeting FtsZ for Antibacterial Evaluation and Mechanistic Study," *European Journal of Medicinal Chemistry* **236** (2022): 114360.
18. Z. Fang, S. Zheng, K. F. Chan, et al., "Design, Synthesis and Antibacterial Evaluation of 2,4-Disubstituted-6-thiophenyl-pyrimidines," *European Journal of Medicinal Chemistry* **161** (2019): 141–153.
19. C. M. Tan, A. G. Therien, J. Lu, et al., "Restoring Methicillin-Resistant *Staphylococcus aureus* Susceptibility to β-Lactam Antibiotics," *Science Translational Medicine* **4**, no. 126 (2012): 126–135.
20. Q. Peng, X. Tang, W. Dong, et al., "Carvacrol Inhibits Bacterial Polysaccharide Intracellular Adhesin Synthesis and Biofilm Formation of Mucoid *Staphylococcus aureus*: An in Vitro and in Vivo Study," *RSC Advances* **13**, no. 41 (2023): 28743–28752.
21. a) F. Bi, L. Guo, Y. Wang, et al., "Design, Synthesis and Biological Activity Evaluation of Novel 2, 6-Difluorobenzamide Derivatives Through FtsZ Inhibition," *Bioorganic & Medicinal Chemistry Letters* **27**, no. 4 (2017): 958–962. b) F. Bi, D. Song, N. Zhang, et al., "Design, Synthesis and Structure-based Optimization of Novel Isoxazole-containing Benzamide Derivatives as FtsZ Modulators," *European Journal of Medicinal Chemistry* **159** (2018): 90–103. c) K. F. Chan, N. Sun, S. C. Yan, et al., "Efficient Synthesis of Amine-Linked 2,4,6-Trisubstituted Pyrimidines as a New Class of Bacterial FtsZ Inhibitors," *ACS Omega* **2**, no. 10 (2017): 7281–7292.

22. R. L. Du, N. Sun, Y. H. Fung, et al., "Discovery of FtsZ Inhibitors by Virtual Screening as Antibacterial Agents and Study of the Inhibition Mechanism," *RSC Med Chem* **13**, no. 1 (2022): 79–89.
23. M. A. Wikler, J. F. Hindler, F. R. Cookerill, J. B. Patel, K. Bush, and M. Powell, *Methods for Dilution Antimicrobial Susceptibility Tests for Bacteria That Grow Aerobically*., Vol. **29**, Clinical and Laboratory Standards Institute, Wayne, PA., 2009, M07–A08.
24. a) J. M. Andreu, C. Schaffner-Barbero, S. Huecas, et al., "The Antibacterial Cell Division Inhibitor PC190723 Is an FtsZ Polymer-stabilizing Agent That Induces Filament Assembly and Condensation," *Journal of Biological Chemistry* **285**, no. 19 (2010): 14239–14246. b) M. Kaul, A. K. Parhi, Y. Zhang, et al., "A Bactericidal Guanidinomethyl Biaryl That Alters the Dynamics of Bacterial FtsZ Polymerization," *Journal of Medicinal Chemistry* **55**, no. 22 (2012): 10160–10176. c) N. Sun, Y. J. Lu, F. Y. Chan, et al., "A Thiazole Orange Derivative Targeting the Bacterial Protein FtsZ Shows Potent Antibacterial Activity," *Frontiers in Microbiology* **8** (2017): 855.
25. a) C. J. Tsai, J. M. Loh, and T. Proft, "Galleria Mellonella Infection Models for the Study of Bacterial Diseases and for Antimicrobial Drug Testing," *Virulence* **7**, no. 3 (2016): 214–229. b) E. Allegra, R. W. Titball, J. Carter, and O. L. Champion, "Galleria mellonella larvae Allow the Discrimination of Toxic and Non-Toxic Chemicals," *Chemosphere* **198** (2018): 469–472.
26. J. Zhang, Z. Chen, X. Huang, et al., "Insights on the Multifunctional Activities of Magnolol," *BioMed Research International* **2019** (2019): 1847130.
27. a) D. Piasecka, M. Braun, M. Mieszkowska, et al., "Upregulation of HIF1-α via an NF-κB/COX2 Pathway Confers Proliferative Dominance of HER2-negative Ductal Carcinoma In Situ Cells in Response to Inflammatory Stimuli," *Neoplasia* **22**, no. 11 (2020): 576–589. b) H. Chen, W. Fu, H. Chen, et al., "Magnolol Attenuates the Inflammation and Enhances Phagocytosis Through the Activation of MAPK, NF-κB Signal Pathways In Vitro and In Vivo," *Molecular Immunology* **105** (2019): 96–106. c) L. Zhang, J. Wang, W. Xu, et al., "Magnolol Inhibits Streptococcus suis-Induced Inflammation and ROS Formation via TLR2/MAPK/NF-kappaB Signaling in RAW264.7 Cells," *Polish Journal of Veterinary Sciences* **21**, no. 1 (2018): 111–118. d) B. Yang, Y. Xu, S. Yu, Y. Huang, L. Lu, and X. Liang, "Anti-angiogenic and Anti-inflammatory Effect of Magnolol in the Oxygen-induced Retinopathy Model," *Inflammation Research* **65**, no. 1 (2016): 81–93. e) M. H. Lin, M. C. Chen, T. H. Chen, H. Y. Chang, and T. C. Chou, "Magnolol Ameliorates Lipopolysaccharide-induced Acute Lung Injury in Rats Through PPAR-γ-dependent Inhibition of NF-kB Activation," *International Immunopharmacology* **28**, no. 1 (2015): 270–278.
28. G. Cheng, M. Hardy, J. Zielonka, et al., "Mitochondria-Targeted Magnolol Inhibits OXPHOS, Proliferation, and Tumor Growth via Modulation of Energetics and Autophagy in Melanoma Cells," *Cancer Treatment and Research Communications* **25** (2020): 100210.
29. F. H. Zhang, H. Y. Ren, J. X. Shen, X. Y. Zhang, H. M. Ye, and D. Y. Shen, "Magnolol Suppresses the Proliferation and Invasion of Cholangiocarcinoma Cells via Inhibiting the NF-kappaB Signaling Pathway," *Biomedicine & Pharmacotherapy* **94** (2017): 474–480.
30. S. F. Hsieh, C. T. Chou, W. Z. Liang, et al., "The Effect of Magnolol on Ca2+ Homeostasis and its Related Physiology in Human Oral Cancer Cells," *Archives of Oral Biology* **89** (2018): 49–54.
31. J. B. Park, M. S. Lee, E. Y. Cha, et al., "Magnolol-Induced Apoptosis in HCT-116 Colon Cancer Cells is Associated With the AMP-Activated Protein Kinase Signaling Pathway," *Biological & Pharmaceutical Bulletin* **35**, no. 9 (2012): 1614–1620.

32. B. T. McKeown, L. McDougall, A. Catalli, and R. A. Hurta, "Magnolol Causes Alterations in the Cell Cycle in Androgen Insensitive Human Prostate Cancer Cells In Vitro by Affecting Expression of Key Cell Cycle Regulatory Proteins," *Nutrition and Cancer* **66**, no. 7 (2014): 1154–1164.
33. J. Shen, H. Ma, T. Zhang, et al., "Magnolol Inhibits the Growth of Non-Small Cell Lung Cancer via Inhibiting Microtubule Polymerization," *Cellular Physiology and Biochemistry* **42**, no. 5 (2017): 1789–1801.
34. a) M. Li, F. Zhang, X. Wang, et al., "Magnolol Inhibits Growth of Gallbladder Cancer Cells Through the p53 Pathway," *Cancer Science* **106**, no. 10 (2015): 1341–1350. b) Y. Liu, W. Cao, B. Zhang, et al., "The Natural Compound Magnolol Inhibits Invasion and Exhibits Potential in Human Breast Cancer Therapy," *Scientific Reports* **3** (2013): 3098. c) M. C. Chen, C. F. Lee, W. H. Huang, and T. C. Chou, "Magnolol Suppresses Hypoxia-induced Angiogenesis Via Inhibition of HIF-1α/VEGF Signaling Pathway in Human Bladder Cancer Cells," *Biochemical Pharmacology* **85**, no. 9 (2013): 1278–1287.
35. a) H. A. Parray, J. Lone, J. P. Park, J. W. Choi, and J. W. Yun, "Magnolol Promotes Thermogenesis and Attenuates Oxidative Stress in 3T3-L1 Adipocytes," *Nutrition* **50** (2018): 82–90. b) K. S. Suh, S. Chon, W. W. Jung, and E. M. Choi, "Magnolol Protects Pancreatic β-cells Against Methylglyoxal-induced Cellular Dysfunction," *Chemico-Biological Interactions* **277** (2017): 101–109. c) L. Pulvirenti, V. Muccilli, N. Cardullo, C. Spatafora, and C. Tringali, "Chemoenzymatic Synthesis and α-Glucosidase Inhibitory Activity of Dimeric Neolignans Inspired by Magnolol," *Journal of Natural Products* **80**, no. 5 (2017): 1648–1657.
36. J. Dong, H. Ding, Y. Liu, et al., "Magnolol Protects Channel Catfish From Aeromonas hydrophila Infection via Inhibiting the Expression of Aerolysin," *Veterinary Microbiology* **211** (2017): 119–123.
37. Y. Sakaue, H. Domon, M. Oda, et al., "Anti-Biofilm and Bactericidal Effects of Magnolia Bark-Derived Magnolol and Honokiol on Streptococcus mutans," *Microbiology and Immunology* **60**, no. 1 (2016): 10–16.
38. S. Oufensou, B. Scherm, G. Pani, et al., "Honokiol, Magnolol and its Monoacetyl Derivative Show Strong Anti-Fungal Effect on Fusarium Isolates of Clinical Relevance," *PLoS ONE* **14**, no. 9 (2019): e0221249.
39. S. V. Nair, G. Baranwal, M. Chatterjee, et al., "Antimicrobial Activity of Plumbagin, a Naturally Occurring Naphthoquinone From Plumbago rosea, Against *Staphylococcus aureus* and Candida albicans," *International Journal of Medical Microbiology* **306**, no. 4 (2016): 237–248.
40. C. Dai, J. Lin, H. Li, et al., "The Natural Product Curcumin as an Antibacterial Agent: Current Achievements and Problems," *Antioxidants* **11**, no. 3 (2022).
41. P. Domadia, S. Swarup, A. Bhunia, J. Sivaraman, and D. Dasgupta, "Inhibition of Bacterial Cell Division Protein FtsZ by Cinnamaldehyde," *Biochemical Pharmacology* **74**, no. 6 (2007): 831–840.
42. J. L. Keffer, S. Huecas, J. T. Hammill, P. Wipf, J. M. Andreu, and C. A. Bewley, "Chrysophaentins are Competitive Inhibitors of FtsZ and Inhibit Z-Ring Formation in Live Bacteria," *Bioorganic & Medicinal Chemistry* **21**, no. 18 (2013): 5673–5678.
43. a) Z. Fang, L. Ban, Y. Li, et al., "A Quinoline-Based FtsZ Inhibitor for the Study of Antimicrobial Activity and Synergistic Effects With β-lactam Antibiotics," *Journal of Pharmacological Sciences* **137**, no. 3 (2018): 283–289. b) D. J. Haydon, N. R. Stokes, R. Ure,

et al., “An Inhibitor of FtsZ With Potent and Selective Anti-Staphylococcal Activity,” *Science* **321**, no. 5896 (2008): 1673–1675.

44. a) N. L. Elsen, J. Lu, G. Parthasarathy, et al., “Mechanism of Action of the Cell-Division Inhibitor PC190723: Modulation of FtsZ Assembly Cooperativity,” *Journal of the American Chemical Society* **134**, no. 30 (2012): 12342–12345. b) Y. Li, J. Hsin, L. Y. Zhao, et al., “FtsZ Protofilaments Use a Hinge-Opening Mechanism for Constrictive Force Generation,” *Science* **341**, no. 6144 (2013): 392–395.

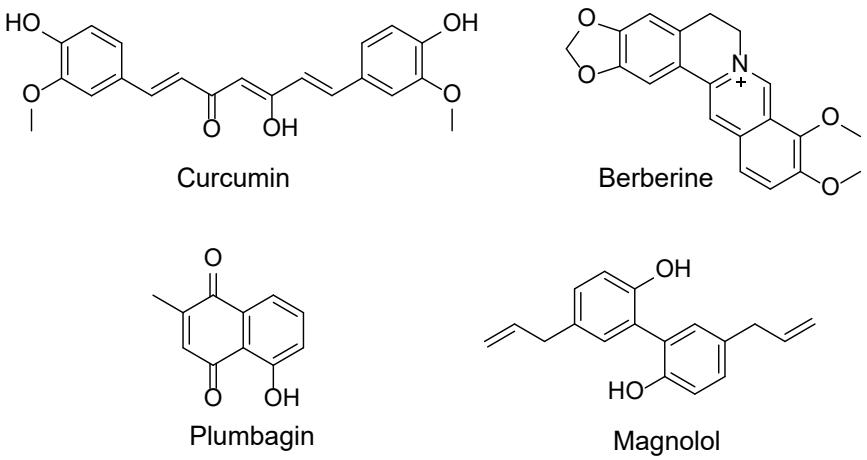

Figure 1. Chemical structures of curcumin, berberine, plumbagin and magnolol.

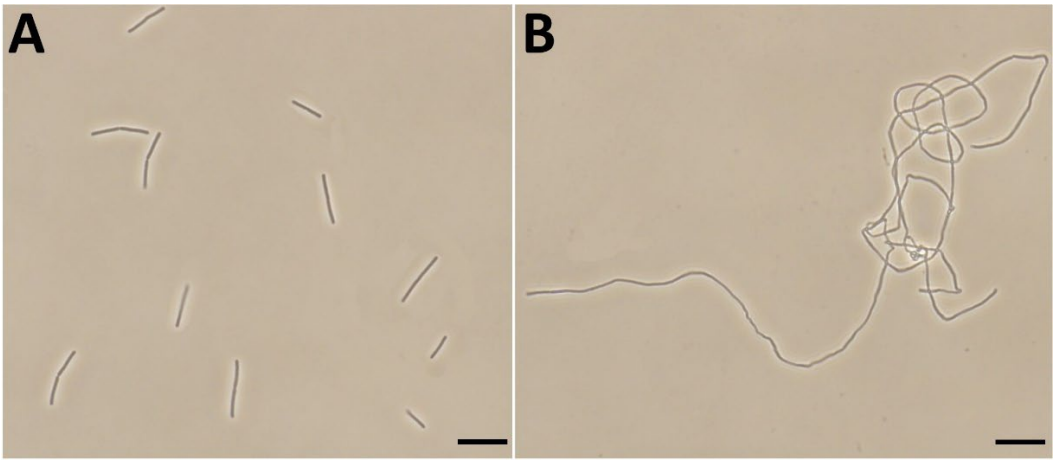

Figure 2. Cell division inhibitory effect of magnolol. Cells of *B. subtilis* 168 were grown in the absence (A), presence of 8 μg/mL of magnolol (B). Scale Bar = 10 μm.

Table 1. Antibacterial activity of magnolol against a panel of bacterial strains.

Bacterial strains	MIC (μg/mL)		
	MG	MET	BER
B. subtilis 168	8	< 1	96
S. aureus ATCC 29213	8	1	192
S. aureus ATCC 29247[a]	8	4	192
S. aureus ATCC 33591[b]	12	1024	192
S. aureus ATCC 33592[b]	12	512	192
S. aureus ATCC 43300[b]	8	512	192
S. epidermidis ATCC 12228	8	0.75	192
E. faecalis ATCC 29212	16	4	> 192
E. faecalis ATCC 51575 [c]	16	4	> 192
E. faecium ATCC 49624	16	4	> 192
E. faecium ATCC 700221[c]	16	4	> 192
E. coli ATCC 25922	> 64	4	> 192
P. aeruginosa ATCC BAA-2108	> 64	> 1024	> 192
K. pneumoniae ATCC BAA-1144	> 64	> 1024	> 192

[a] ampicillin-resistant strain; [b] MRSA; [c] Vancomycin-resistant strains; MG denotes magnolol; MET denotes methicillin; BER denotes berberine.

Table 2. The MBC (μg/mL) of magnolol against the selected bacterial strains.

Bacterial strains	MBC	MIC	MBC/MIC
B. subtilis 168	8	8	1
S. aureus ATCC 29213	16	8	2
S. aureus ATCC 43300	16	8	2
E. faecium ATCC 700221	16	16	1

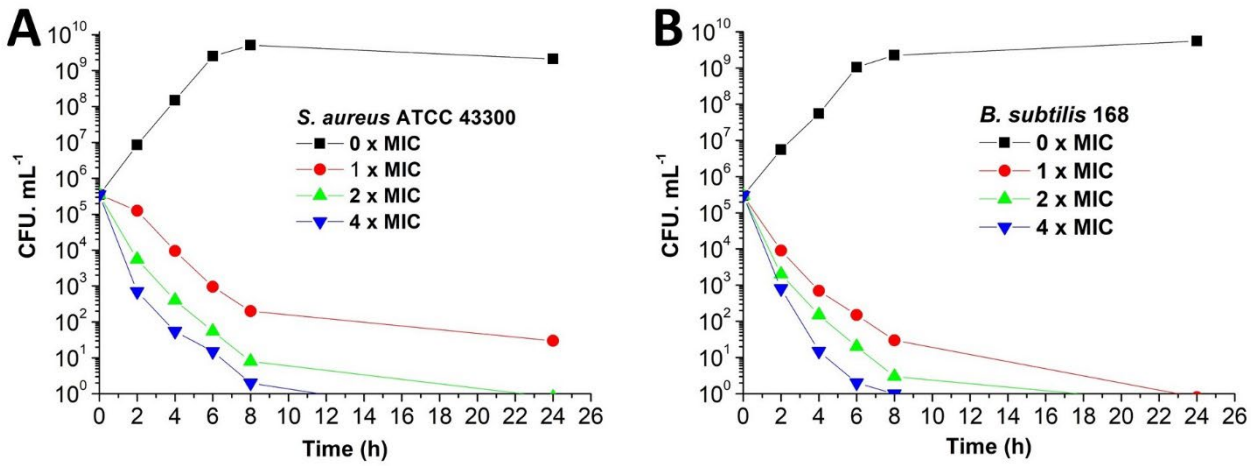

Figure 3. Time-killing curves of magnolol. Samples of a growing culture of *S. aureus* ATCC 43300 (A) and *B. Subtilis* 168 (B) were incubated with concentrations of magnolol equivalent to 1× (red), 2× (green), or 4× (blue) the MIC. Vehicle (1% DMSO; black) was included.

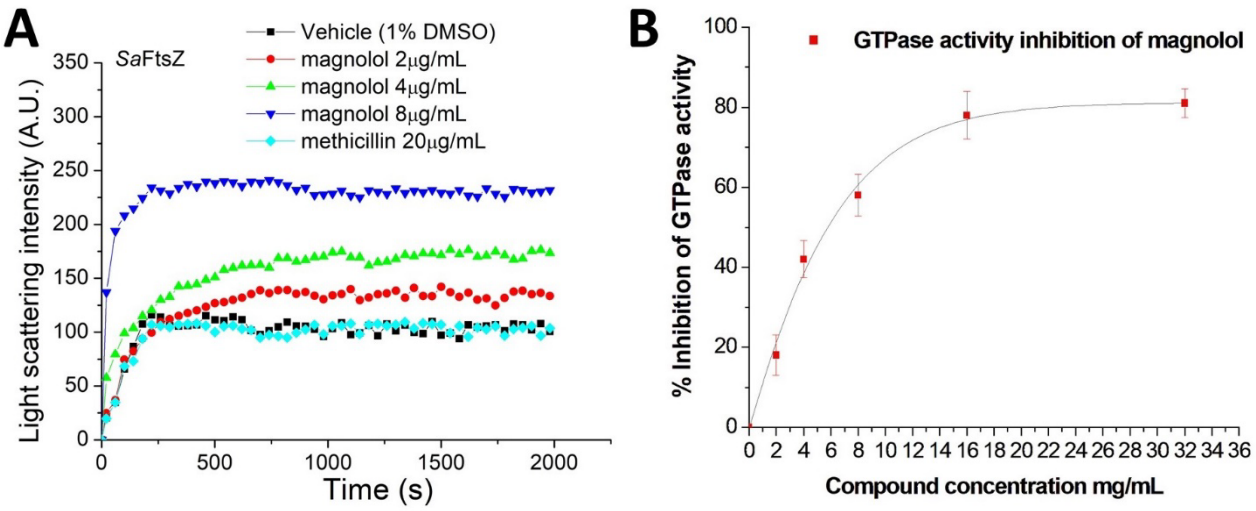

Figure 4. *In vitro* effects of magnolol on the FtsZ. (A)Time-dependent polymerization profiles of FtsZ in the absence and presence of magnolol at a concentration range from 2 to 8 μg/mL. (B) Inhibition of GTPase activity of FtsZ by magnolol.

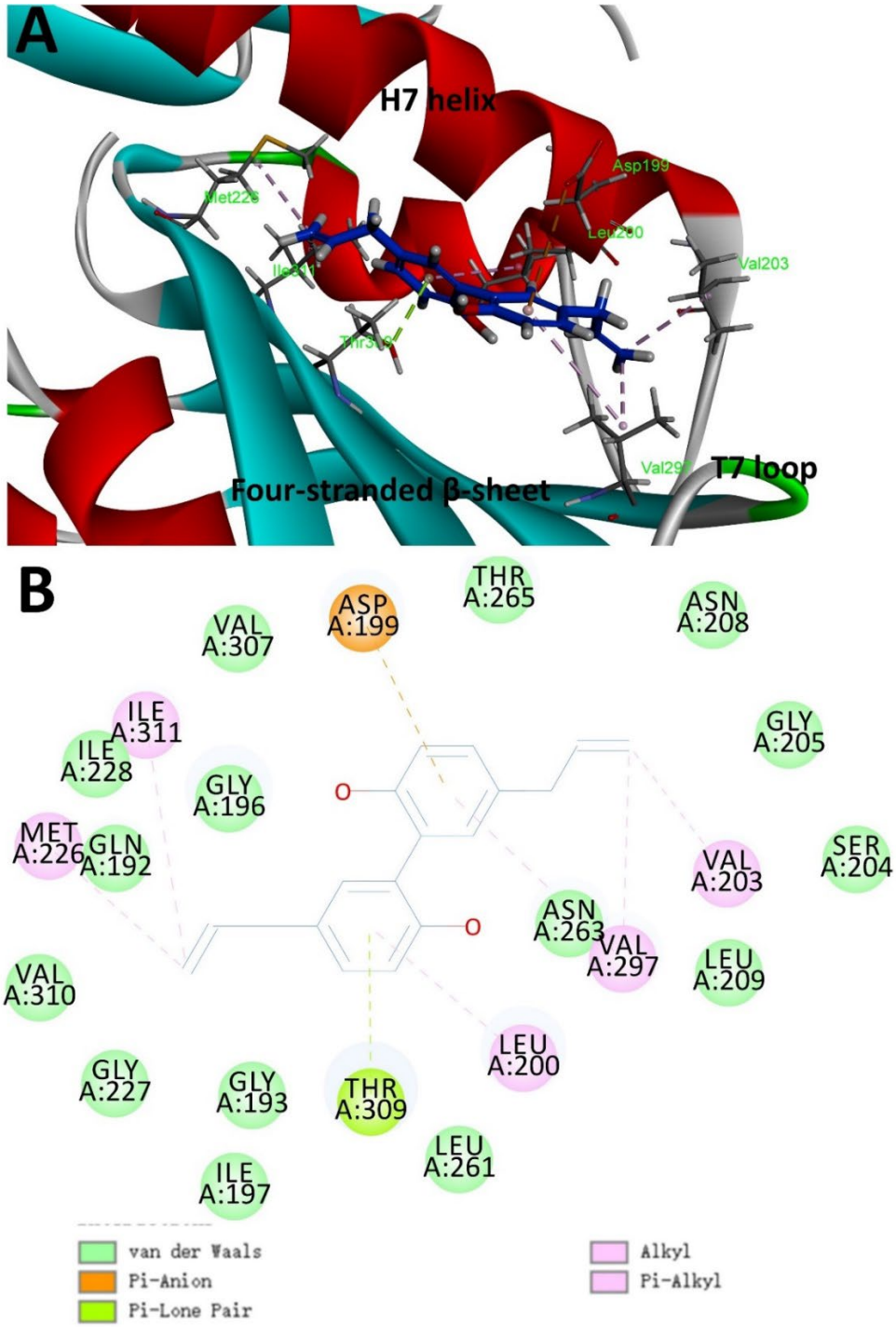

Figure 5. The proposed binding mode of magnolol in *S. aureus* FtsZ (PDB ID: 4DXD). (A) Magnolol in the interdomain cleft of FtsZ; (B) Predicted interaction between magnolol and amino acids of FtsZ.

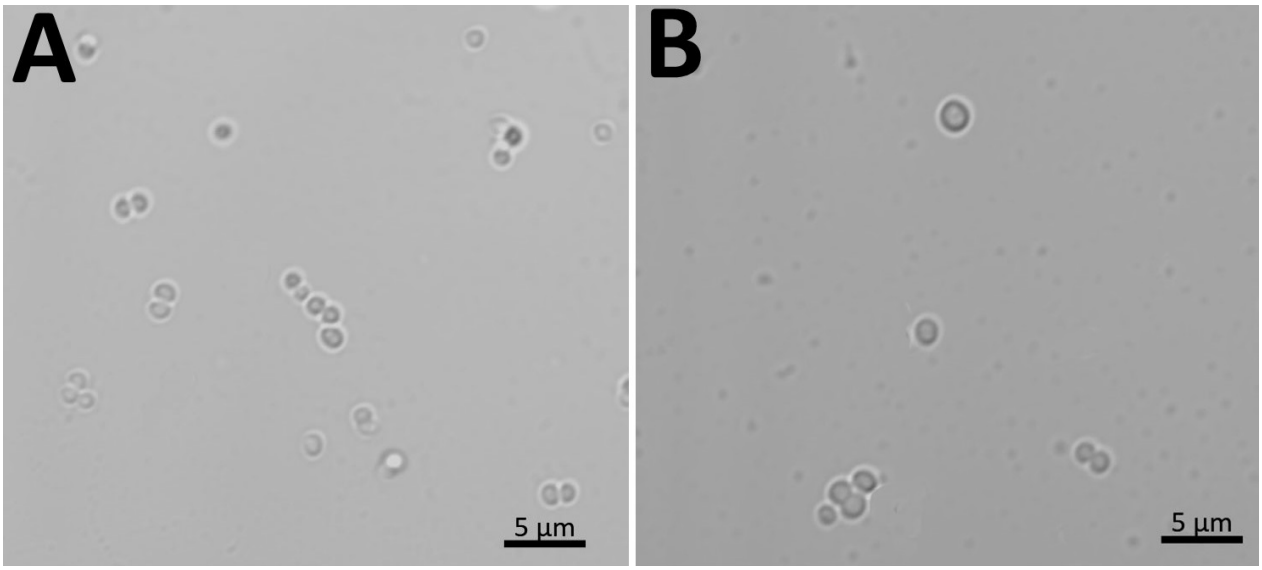

Figure 6. Cell division inhibitory effect of magnolol. Cells of *S. aureus* ATCC 29213 were grown in the absence (A), presence of 8 μg/mL of magnolol (B). Scale Bar = 5 μm.

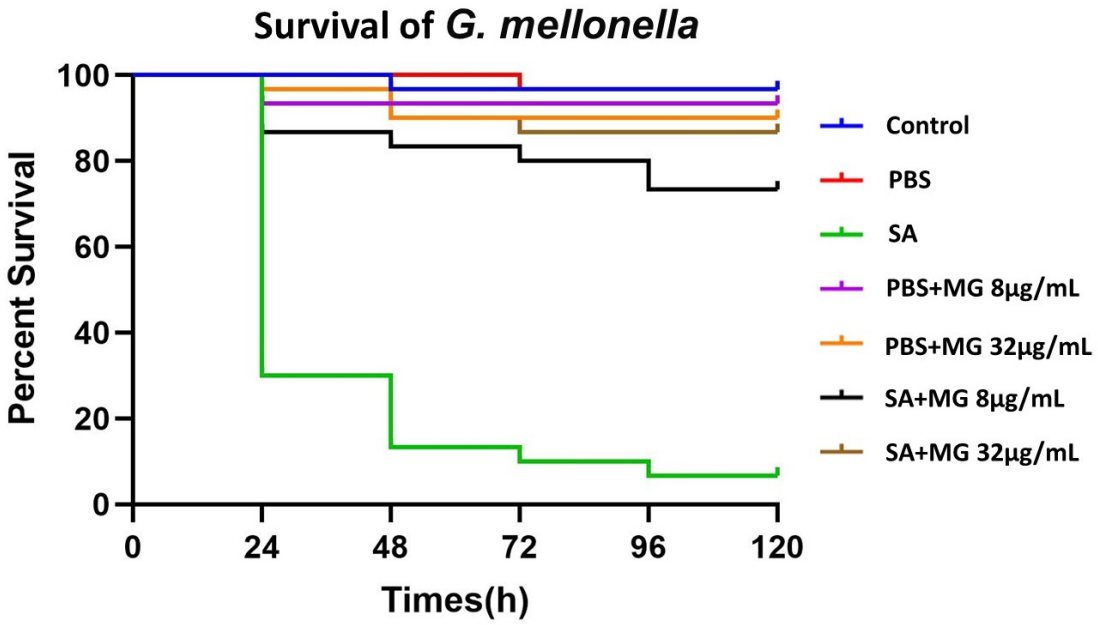

Figure 7. Evaluation of the toxicity and antibacterial activity of magnolol *in vivo via* using the *G. mellonella* larvae models (MG: magnolol; 29213: *S. aureus* ATCC 29213).